International Journal of Fluid Machinery and Systems
Vol. 2, No. 4, October-December 2009

Original Paper (Invited)

Large Eddy Simulation of a High Reynolds Number Swirling Flow in a Conical Diffuser

Cédric Duprat[1], Olivier Métais[1] and Thomas Laverne[2]

[1]LEGI INPG CNRS – Modélisation et Simulation de la Turbulence (MoST)
1025, rue de la piscine, Grenoble, 38041, France,
cedric.duprat@grenoble-inp.fr, olivier.metais@grenoble-inp.fr
[2]Alstom HYDRO FRANCE
89, av. Léon Blum, Grenoble, 38000, France, Thomas.laverne@power.alstom.com

Abstract

The objective of the present work is to improve numerical predictions of unsteady turbulent swirling flows in the draft tubes of hydraulic power plants. We present Large Eddy Simulation (LES) results on a simplified draft tube consisting of a straight conical diffuser. The basis of LES is to solve the large scales of motion, which contain most of the energy, while the small scales are modeled. LES strategy is here preferred to the average equations strategies (RANS models) because it resolves directly the most energetic part of the turbulent flow. LES is now recognized as a powerful tool to simulate real applications in several engineering fields which are more and more frequently found. However, the cost of large-eddy simulations of wall bounded flows is still expensive. Bypass methods are investigated to perform high-Reynolds-number LES at a reasonable cost. In this study, computations at a Reynolds number about 2 10^5 are presented. This study presents the result of a new near-wall model for turbulent boundary layer taking into account the streamwise pressure gradient (adverse or favorable). Validations are made based on simple channel flow, without any pressure gradient and on the data base ERCOFTAC. The experiments carried out by Clausen et al. [1] reproduce the essential features of the complex flow and are used to develop and test closure models for such flows.

Keywords: Large-Eddy Simulation, Near-wall scaling, Swirling flows, CFD.

1. Introduction

The flow downstream an hydraulic turbine is a swirling flow which presents a strong unsteady vortex core within the draft tube. It may trigger instabilities whose development has serious impacts on the efficiency of the system. The draft tube is also sensitive to flow separation due to the presence of a strong pressure gradient. It is still a great challenge to numerically reproduce the flow dynamics and to predict the associated instabilities. The purpose of the present study is a first step towards the numerical simulation of a full draft tube configuration: we here consider a simplified draft tube consisting of a straight conical diffuser. This flow exhibits most of the complex features of a draft tube: presence of swirl generated by unsteady inflow conditions, high Reynolds number and adverse pressure gradient which may eventually lead to flow separation. The code validation was based on an ERCOFTAC data base which provides accurate experimental data even close to the wall [1]. The experiments reproduce the essential features of the complex flow and are here used to test the numerical procedure and the modeling assumptions. Since high Reynolds numbers are here involved, the goal of the present study is to test the wall modeling procedure originally proposed by Manhart *et al.* [2] which has the ability to take into account the presence of local pressure gradients and is therefore suitable to reproduce accurately flow separation.

The first section of this study deals with the methodology we used. Details of the numerical experiments; the turbulent model and then the code used are given. Then, we develop the near-wall scaling for turbulent boundary layers with adverse pressure gradient we used; the theory and first validation test case which is a periodic channel flow. In the last part is developed the second test case geometry, its mesh and its boundary condition. In particular, we focused on the inflow condition which is a crucial point in LES. Because we solve unsteady turbulent flow, the inflow within the diffuser, need to be as realistic as possible. Hence, an adequate representation of the inflow conditions has been developed and is explained here to reproduce the experimental inflow.

In the second section of the present work, we show the obtained results with the diffuser test case. We finish by comments about the diffuser test case.

Accepted for publication May 27 2009: Paper number O09034S
Corresponding author: Cedric Duprat, Dr., Cedric.Duprat@hmg.inpg.fr

This manuscript was presented at the 24th IAHR Symposium on Hydraulic Machinery and Systems, October 27-31, 2008, Foz do Iguassu-Brazil.

2. Methodology

2.1 Numerical experiment

We use the newly distributed open source CFD code based on the Field Operation and Manipulation C++ class library for continuum mechanics (OpenFOAM, *http://www.opencfd.co.uk*). The Navier-Stokes equations are solved for turbulent incompressible flow with a polyhedral finite-volume approach. It is both implicit and explicit second-order Finite Volume code. Our three dimensional computations are second order accuracy in both time, from Crank-Nicholson scheme, and space, from central scheme. This freeware was already evaluated for turbulent flow in water turbines and was proved to be comparable with major commercial CFD tools ([3], [4]). The C++ code library of classes includes a well-tested and validated large-eddy simulation capability [5]. In the LES method, large-scale are numerically resolved whereas small-scales are modeled by a well chosen sub-grid scale model. It is an extremely powerful technique for unsteady flow, since it describes explicitly all the energy containing scales of the flow.

2.2 Turbulence modeling

The governing equations for the large eddy simulation of incompressible fluid, which have been convolutes with a filter of uniform width Δ, are given by:

$$\nabla.\bar{u} = 0, \tag{1}$$

$$\frac{\partial \bar{u}}{\partial t} + \nabla.\left(\bar{u}\bar{u}\right) = -\frac{1}{\rho}\nabla.\bar{p} + \nabla.\nu\left(\nabla\bar{u} + \nabla\bar{u}^{T}\right) + \nabla.\tau, \tag{2}$$

Here, $\bar{u}$ is the filtered velocity, ρ is the fluid density, $\bar{p}$ the filtered pressure, ν the cinematic viscosity and τ the sub-grid scale (SGS) stress tensor which has to be modeled to close the system.

Modeling the small-eddy of the flow leads to find a correct sub-grid scale (SGS) viscosity. We choose to get the SGS viscosity from a transport equation for the sub-grid scale turbulent energy, which is assumed to be isotropic. Adding an history effect, such as a transport equation let us take bigger cells size for the grid. Compare to the Smagorinsky model, where we impose a constant turbulent viscosity in each cell, we here transport the information inside each cell which is more accurate in coarse grid region.

The transport equation for the sub-grid kinetic energy is given by the following equation:

$$\overbrace{\frac{\partial k_{SGS}^2}{\partial t}}^{time} + \overbrace{\frac{\partial}{\partial x_j}\left(k_{SGS}^2\bar{u}\right)}^{convection} - \overbrace{\nabla.\left[\left(\nu+\nu_{SGS}\right)\nabla k_{SGS}^2\right]}^{diffusion} = \overbrace{-\varepsilon - \tau:\bar{S}}^{sources} \tag{3}$$

Where the SGS eddy-viscosity ν_{SGS} , and the dissipation ε, can be found from,

$$\begin{aligned} \nu_{SGS} &= C_k k_{SGS}^{1/2}\Delta \\ \varepsilon &= C_\varepsilon \frac{k_{SGS}^{3/2}}{\Delta} \end{aligned} \tag{4}$$

As the normal stresses are taken as isotropic and can therefore be expressed in terms of the SGS kinetic energy, the following equations close the system;

$$\tau - \frac{1}{3}tr\left(\tau\right)I = \tau - \frac{2}{3}k_{SGS}^2 I = -\nu_{SGS}\left(\nabla\bar{u} + \nabla\bar{u}^{T}\right) \tag{5}$$

The isotropic part of the stress tensor $\frac{1}{3}tr\left(\tau\right)$, is either modeled or expressed in the filtered pressure. A study of the performance of different SGS models in channel flows by Fureby *et al.* [5] has shown the one-equation model to be quite effective and superior to algebraic relations such as the Smagorinsky model in flows with large scale unsteadiness. In the wall proximity region, they generally find that models involving transport equations generate better profiles than purely algebraic models.

2.3 Wall modeling approach

There are many strategies for wall modeling in LES. The model we used can be classified as an Equilibrium Stress Model (ESM). We assume that the stresses in the boundary layer are in some kind of average or instantaneous equilibrium. This model uses an approximate correlation to specify the wall shear stresses as a function of local velocity and local pressure gradients at the first off-the-wall grid point. To take pressure gradient into account, a pressure based quantity $u_p = \left|\frac{\mu}{\rho^2}\frac{\partial p}{\partial x}\right|^{1/3}$ and a combined velocity $u_{\tau p} = \sqrt{u_\tau^2 + u_p^2}$ has been defined. In the previous velocity, u_τ is the classic friction velocity. The following new near-wall scaling is used for velocity [2]:

$$u^*\left(y^*\right) = sign\left(\tau_w\right)\alpha y^* + sign\left(\frac{\partial p}{\partial x}\right)\frac{1}{2}\left(1-\alpha\right)^{3/2} y^{*2} \tag{6}$$

With the reduced velocity u^*, expressed in wall units is defined as : $u^* = \frac{u}{u_{\tau p}}$ and $y^* = \frac{y u_{\tau p}}{\nu}$. The ratio $\alpha = \frac{u_\tau^2}{u_{\tau p}^2}$ quantifies which effect, friction or pressure gradient, is preponderant. Hence, if at one point of the grid $\alpha = 0$, there is a flow separation at this point. If $\alpha = 1$ there is no pressure gradients effect at considered the grid point.

A second assumption was done; the first off-the-wall cell has to be in the viscous sublayer, which means that $y^* < 7$. Notice that from the previous equation, if there is no pressure gradients effect, the well known linear expression for the velocity $\left(u^+ = y^+\right)$ is recovered. To validate the previous implementation, a LES of a fully developed turbulent flow in a plane channel at Re_τ=395 ($Re_\tau = u_\tau * h/\upsilon$, h channel half width) is considered. The influences of different wall unit are compared together and with the Direct Numerical Simulation (DNS) of Moser [6]. The computational domain is 2π in streamwise direction (x), 2h in wall normal direction (y) and πh in spanwise direction (z). The walls are treated as no-slip boundaries. The streamwise (x) and spanwise (z) directions are formally infinite.

Assuming that the fully developed flow is homogeneous, periodic boundary conditions can be applied in streamwise and spanwise direction to avoid problems associated with inflow and outflow conditions. The flow is initialized using a laminar parabolic profile (a simple Poiseuille profile). Near-wall parallel streaks of slow and faster moving fluid are produced by modifying this initial parabolic flow adding a sinusoidal perturbation in both streamwise and spanwise direction [7]. The solution of the plane channel will now rapidly become turbulent as the sinuous streaks induce vortex formation and further instability.

2.4 Inflow condition

To reduce the cost of the computation, synthetic but realistic inflow conditions have to be economically generated. It is well known that the inflow boundary condition can have a strong influence, not only in the vicinity of the inlet but also for the entire flow development. For purely longitudinally orientated mean flows various techniques can be applied: one can use periodic boundary conditions if the flow is homogeneous in the flow direction or recycling techniques to reinject the outflow at the inflow with a proper rescaling. Because these spatially periodic flows are not self-sustaining, a body force has to be added to maintain a constant mass flow rate. The axial body force used to keep the mass flow rate, represents the mean pressure gradients that drives the physical flow. In the presence of swirl, it is slightly trickier to maintain both the longitudinal and the azimutal flow rate. Landman proposed a method [8] to deal with the azimuthal direction by applying the following body force $f_\theta(r)$ in DNS calculation:

$$f_\theta\left(r\right) = \frac{F}{\left[1 + \left(\frac{r}{r_0}\right)^2\right]^2}, \tag{7}$$

where F is a constant scaling factor that determines the overall strength of the applied body force. Hence, F is calculated dynamically at each time step to "push" the flow at the target Swirl number fixed by the user. Landman's forcing term has not yet been tested in LES; we therefore used this body force combined with the pressure gradients to keep both swirl number and mass flow rate.

To validate this methods for generating the inflow condition, we chose to generate a controlled swirling flow in a straight pipe, L=10D where L is the length of the pipe and D its diameter. Reynolds number is fixed at 2.02 10^5 which correspond to the same Reynolds number as the experimental axisymetric diffuser.

As for the previous channel flow calculation, we started from a Poiseuille flow without any swirl. The superimposed random disturbances perturb the flow after a few crossing of the flow, making it fully turbulent. Turbulent structures appear in the flow after a few crossing-time (fig.1). Initial streamwise velocity profile can be compare to the 100 cross-flow streamwise velocity profile (fig. 2, right). We can recognize respectively a laminar and a turbulent profile. The dynamic procedure to keep the mass-flow average and the swirl number generate a tangential velocity which changes dynamically at each time step by the body force (fig. 2, left).

Fig. 1: Instantanious velocity: initial (left), after 100 cross-flow (right) in the diametral plane and a cross section

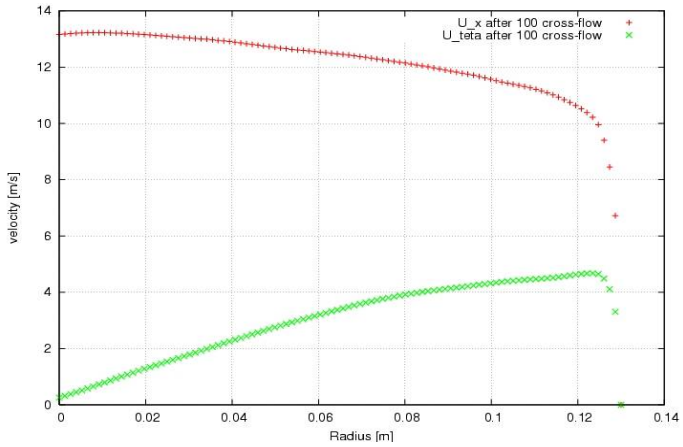

Fig. 2: Two components of the velocity profile after 100 cross flow

Instantaneous iso-surfaces of the second invariant of the velocity gradient, Q are showed (fig. 3). We compare the previous calculation with a 5D length periodic pipe at the same Reynolds number and with the same grid density. Figure 3 shows that the patterns of the flow, considering the turbulent structures, are really different. A short pipe generates a double-helix structure which is stable along the run. Because of the periodicity, the flow is constrained in its length and structures can appear in some case but not in other case despite the concept of periodic flow. To reproduce the axisymetric test case inflow, these descriptions have to be taken into account

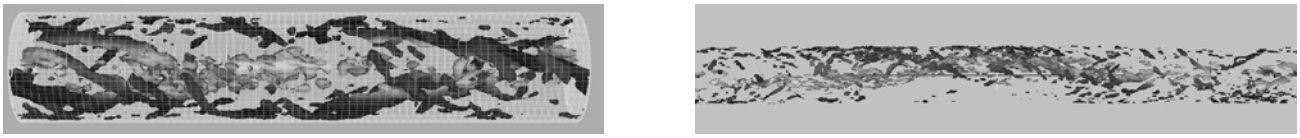

Fig. 3: Visualizations of the flow structure in a periodic swirling pipe flow:
L=5D pipe (left), L=10D pipe (right), by the Q criterium

The parameters S_w and the bulk velocity U_{bulk} let us control the flow in the pipe. We will use this procedure for the inlet boundary condition of the axisymetric diffuser.

3. Results on the axisymetric diffuser

3.1 Description of the test case

To use a minimal storage overhead, a single geometry is used to create the inflow and to model the test case geometry. The mapped inlet method employs a simple scaled mapping of the velocity field from some plane in the interior of the domain (fig. 4, left). Hence, the scaling plane is used to specify bulk flow rate (by U_{bulk}) and the swirl (by S_w).

The grid considered for this case consists of 2 10^6 nodes. Focusing on the most interesting part of the domain, inlet generator and the diffuser consist of 2/3 of the total number of nodes. We use wall-normal stretching to keep $y^+ < 10$ in the pipe before the diffuser. The reason is that the boundary layer concentrates velocity gradients in a thin near-wall region in this pipe. This region rapidly grows thicker under the influence of the negative pressure gradients in the diffuser. So this first point off-the-wall is enough to calculate shear stress and pressure gradient with previous wall model.

The length of the mapping part in reduces to L=2D to keep agreement with previous calculations ([10], [11]). Like for the inlet validation, this has a consequence on the big size structure at the inlet, a stable rectilinear vortex (fig. 6, right) (Vortex filament) can be seen which correspond to a different flow regime from previous pipe calculations.

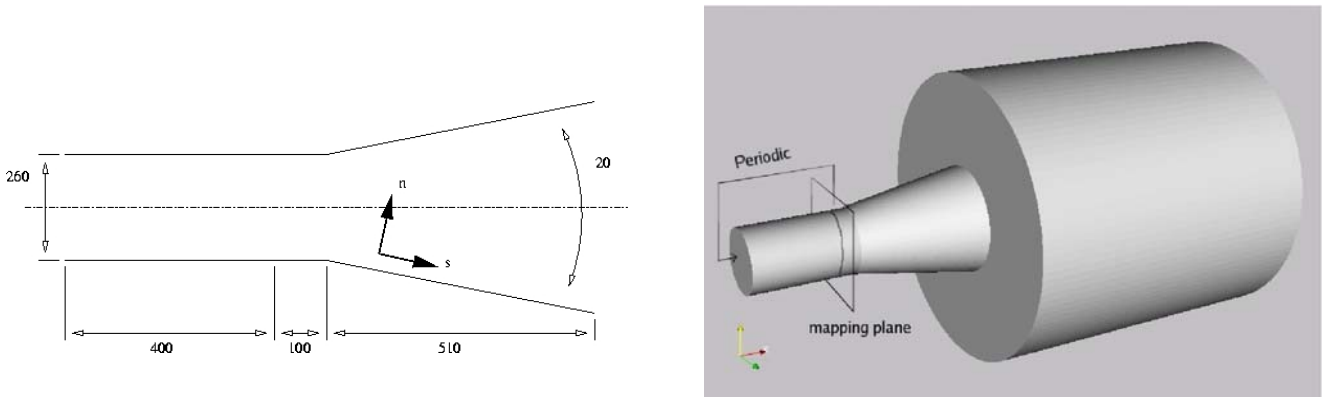

Fig. 4: Geometry of the diffuser: experimental geometry from Clausen [1] (left),
numerical geometry with the pipe at the amount of the diffuser and the bulk after the diffuser (right)

3.2 Instantaneous results

An instantaneous realization of the diffuser velocity and diffuser kinetic energy distribution in the x - y plane can be seen in figure (5). Although not as representative as a time mean plot, they do convey a more intuitive feel for the scales and structures present in the diffuser flow. Elevated values of SGS kinetic energy are normally associated with large resolved scale stresses. High values of K along the diffuser at the entrance to the expansion are a product of a very strong rapidly fluctuating shear layer in this region. The axisymetric axis along the diffuser is also an area of stresses generation. This area corresponds to a large eddy vortex rotating at a low frequency around the axis. This vortex is generated by flow separations at the wall. Flow stream lines are perturbed by the separation point and this pattern lead to a variation of pressure gradients. The streamwise instantaneous velocity picture shows this shift of the main flow. Large scale mixing is visible as inclusions of slower moving fluid penetrating into the faster stream and *vice versa*. The sudden change from cylindrical pipe to diffuser necessitates a rapid change of the flow pattern.

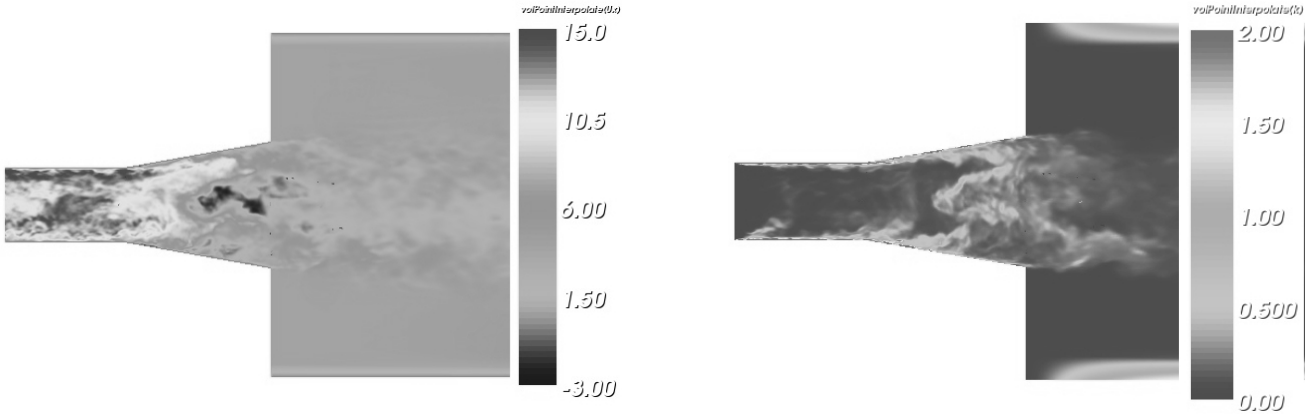

Fig. 5: LES instantaneous streamwise velocity in the entire domain (left), kinetic energy in the diffuser section (right)

In an axisymetric geometry, adding swirl delayed separation point. The swirl quantity was initially defined by the experiments to avoid both separation and recirculation in the flow. It is not the case on all the circumference of the diffuser at each time step. Flow separation takes place in a helix at the diffuser wall. Streamline go around this recirculation and that create the recirculation in the center of the diffuser. Because separation's shape is an helicoidal, the recirculation in the center of the diffuser will also rotate which explain its helical shape. Such results can't be found by statistical turbulence model because of the average procedure which will erase these unsteady flow patterns.

Two hypotheses can explain the difference between experiments and the computational result. First, the present result can represent the end on the transitory part. Because we start from a simple Poiseuille flow without swirl, swirl number parameter increase up to the experimental one, then, some oscillations appear around the focus swirl number. Wait for the stationary part of the calculation will show if the separation still occurred or not. The second hypothesis is about the experimental techniques, Clausen sampled single hot wires at 1 kHz for 30s to get his results. Hot wires give absolute value of the velocity component, so it's not possible to extract the sign of the velocity. Because the separation's shape is helicoidal, the 30s of sampling may be too much and play as a filter of the negative velocity values.

3.3 Structures inside the diffuser

Focusing on the vortices along the wall of the geometry (Fig. 6), interesting features are revealed. From the left to the right, the images show *a)* iso-pressure contour for two different values of the pressure, *b)* iso-value of the Q criterion. The two images show, at the same time, two different sizes of vortices we are able to visualize in LES. The pressure iso-contour is a large scale vortex,

rotating at low frequency. The vortex is stable in amount of the diffuser and become, due to separation, unsteady. We can find such pattern in RANS calculation but without details in the shape of the vortex. The iso-value of Q criterion gives smaller details in scale, which is characteristic to LES calculation. These vortices, very close to the wall in the amount of the diffuser, are stretched in the diffuser due to pressure gradient. This also confirms that the boundary layer is much more strongly attached in the upper region than in the diffuser, where more turbulence production is clearly occurring.

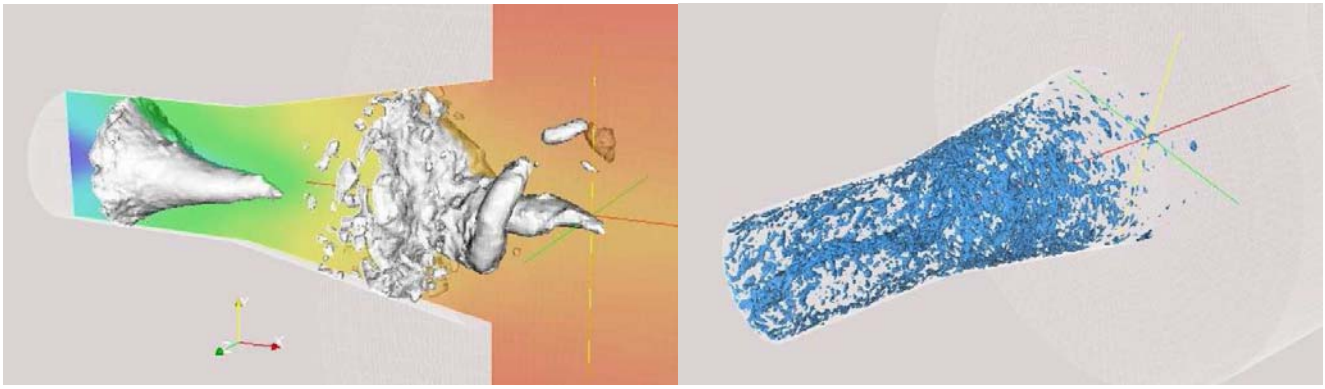

Fig. 6: LES instantaneous turbulence properties in the diffuser: iso-pressure contours low pressure, low pressure for the left one and higher pressure for the right one (left), resolved vortical structures visualized via iso-surface of Q >6e+5

4. Final considerations

One of the aims of this work was to evaluate the OpenFOAM CFD tool for LES in a complex geometry at high Reynolds number. To reach this objective, an effective wall modeling, taking into account both of shear stress and pressure gradient, has been implemented. Adapted numerical method were also use to reduce the cost, keeping an accurate result for such Reynolds number. One outcome of this evaluation is that OpenFOAM is able to generate good computational LES results. The other is that numerical procedure for wall modeling and generation of turbulent inlet give preliminary results indicating a good physical agreement.

Acknowledgments

This work is part of Tenerdis project which let a collaboration between the ADEME (French Environment and Energy Management Agency) and ALSTOM Hydro Power and INPG (Grenoble institute of Technology). The active OpenFOAM community is gratefully acknowledged for sharing their time and their knowledge.

Nomenclature

C_ε; C_k	LES sub-grid scale model constant [-]	u_τ	Friction based velocity [m/s]
f_θ	Orthoradial body force [N]	$u_{\tau p}$	Characteristic velocity [m/s]
k_{SGS}	Sub-grid kinetic energy	u_i	Instantaneous velocity components (i=1, 2, 3)[m/s]
P	Pressure [Pa]	u*	
r	Radius direction [m]	y*	Non-dimentional velocity [-]
r_0	Inlet radius [m]	Δ	Non-dimensional length [-]
Re_τ	Reynolds number based of the friction velocity [-]	ν_{SGS}	Sub-grid characteristic length [m]
S	Deviatoric part of the velocity gradient tensor	ρ	Sub-grid scale eddy viscosity
u_p	Pressure based velocity [m/s]	τ	Fluid Density [kg/m^3]
			Shear stress tensor

References

[1] Clausen, D.H., Wood, D.H., and Koh, S.G., 1992, "Measurements of a swirling turbulent boundary layer developing in a conical diffuser," Experimental Thermal and Fluid Science, Vol. 6, No. 2, pp. 39-48.

[2] Manhart, M., Peller, N., and Brun, C., 2008, "Near-wall scaling for turbulent boundary layers with adverse pressure gradient," Theoretical Comput. Fluid Dynamic, Vol. 22, No. 2, pp. 243-260.

[3] Nilsson, H., 2006 "Evaluation of OpenFOAM for CFD of turbulent flow in water turbines," IAHR Symposium on Hydraulic Machinery and Systems, Yokohama, Japan

[4] Page, M. and Beaudoin, M., 2007 "Adapting OpenFOAM for turbomachinery applications," 2nd OpenFOAM Workshop Zagreb, Croatia

[5] Fureby, C., Tabor, G, Gosman, A.D., and Weller, H.G., 1997 "A comparative study of subgrid scale models in homogeneous isotropic turbulence," Physic of Fluid Vol. 9, No. , pp. 1416-1429

[6] Moser, R.D., Mansour, N.N., and Kim, J., 1999 "Direct numerical simulation of turbulent channel flow up to $\mathrm{Re}_\tau = 590$," Physic of Fluid Vol. 11, No. 4, pp. 943-945

[7] Schoppa, W. and Hussain, F., 2000 “Coherent structure dynamics in near-wall turbulence,” Fluid Dynamics Research Vol. 26, pp. 119-139
[8] Landman, M.J., 1990 “On the generation of helical waves in circular pipe flow,” Physic of Fluid, Vol. 2, No. 5, pp. 738-747
[9] Orlanski, I., 1976 “A simple boundary condition for unbounded hyperbolic flows,” Journal of Computational Physics, Vol. 21, No. 3, pp. 251-269
[10] Gyllenram, W. and Nilsson, H., 2004 “Numerical investigations of swirling flow in a conical diffuser,” 22 IAHR Symposium on Hydraulic Machinery and Systems, Stockholm, Sweden
[11] Armfield, S.W., Cho, N.-H., and Fletcher C.A.J., 1990 “Prediction of turbulence quantities for swirling flow in conical diffusers,” AIAA, Vol. 28, No. 3, pp. 453-460